Simulation and Performance of the Pan-European Land Mobile Radio System

Giovanna D'Aria, Flavio Muratore, and Valerio Palestini

Abstract— **The introduction of the ETSI/GSM digital land mobile radio system has required the study and application of advanced transmission techniques, necessary to meet the quality objectives in very demanding environments. In particular, this paper considers the performance of the compact-spectrum constant-envelope modulation chosen by European Telecommunications Standards Institute/Groupe Special Mobiles (ETSI/GSM), together with concatenated block and convolutional coding, Viterbi adaptive equalization, and soft-decision Viterbi decoding to cope with the severe time- and frequency-selective distortions caused by propagation phenomena, properly modeled for computer simulation. Channel coding and adaptive equalization techniques, supported also by frequency hopping and diversity reception, are fundamental to operate the system with the required quality.**

I. Introduction

In the second half of 1991 the digital land mobile radio system specified by ETSI/GSM (European Telecommunications Standards Institute/Groupe Special Mobiles) will have been put into service in several European countries. The achievement of this goal has necessitated the solution of a number of problems, due to the following:

1) this will be the first all-digital system with frequency division multiple access/time division multiple access (FDMA/TDMA) in the mobile-to-base link and time division multiplexing (TDM) in the base-to-mobile link;
2) it operates in the 900 MHz frequency band (890–915 MHz for the mobile-to-base link and 935–960 MHz for the base-to-mobile link),
3) each carrier, spaced by 200 kHz, supports eight traffic channels, with gross bit rate of 270.83 kb/s;
4) the cellular coverage of the service area envisages sophisticated signaling, protocols, and control channels;
5) to increase the system capacity, a low-redundancy digital speech code has been selected, e.g., regular pulse excited–long-term prediction (RPE-LTP) with a bit rate of 13 kb/s, requiring a selective bit protection against transmission errors;
6) to increase both spectrum and power-consumption efficiency, a compact-spectrum constant-envelope modulation technique has been adopted;
7) severe propagation conditions have to be coped with, such as those typical of urban and suburban areas, hilly and mountainous areas, with vehicle speeds up to about 250 km/h;
8) to meet the quality constraints, it is necessary to adopt sophisticated channel coding (block and convolutional codes) and adaptive equalization techniques (either maximum likelihood sequence estimation (MLSE) or transversal filtering with Kalman adaptation), together with frequency hopping and diversity reception.

In this paper, we present a performance evaluation (by computer simulation) of the radio transmission system, considering the modulation and channel coding characteristics as specified by ETSI/GSM, and using a Viterbi algorithm approach to the MLSE adaptive equalization. In this regard, both time- and frequency-selective distortions due to propagation are considered, and a modeling and computer simulation technique is addressed.

Manuscript received June 28, 1991. This work was supported by SIP, the Italian Telephone Operating Company.

The authors are with the Radio Systems Department, Centro Studi e Laboratori Telecomunicazioni (CSELT), 10100 Torino, Italy.

IEEE Log Number 9105605.

II. Transmitter Characteristics

ETSI/GSM has specified the performance of the radio channels and the transmitter characteristics, for compatibility purposes on the radio interface; on the other hand, the receiver implementation can be chosen by manufacturers for the best trade-off between performance and cost.

Two traffic and two control channels specified by GSM in [1] and described in what follows have been simulated; in particular, the traffic channels refer to a speech and to a data channel while the control channels refer to a stand-alone dedicated channel and to a synchronization channel.

The simulations have been carried out by means of a software package named TDMAGSM, developed at CSELT by revising and specializing a more general software for TDMA system simulation named TDMASIM [2]. This program is capable of simulating the overall radio chain specified by GSM, including co-decoding, mo-demodulation, adaptive equalization, and propagation effects [3], [4], as illustrated in Fig. 1. The simulated chain includes the blocks relevant to the arrangement of the digital stream [1] (such as coding, reordering and partitioning, interleaving, and burst formatting), modulation, propagation, interferences, synchronization, demodulation, adaptive equalization, and decoding.

The GSM modulation is a Gaussian minimum shift keying (GMSK) modulation with differential-type precoding and B·T product equal to 0.3 and bit rate of 270.83 kb/s [5].

A. Speech Channel at Full Rate (TCH/FS)

In the case of the speech channel at full rate (13 kb/s),

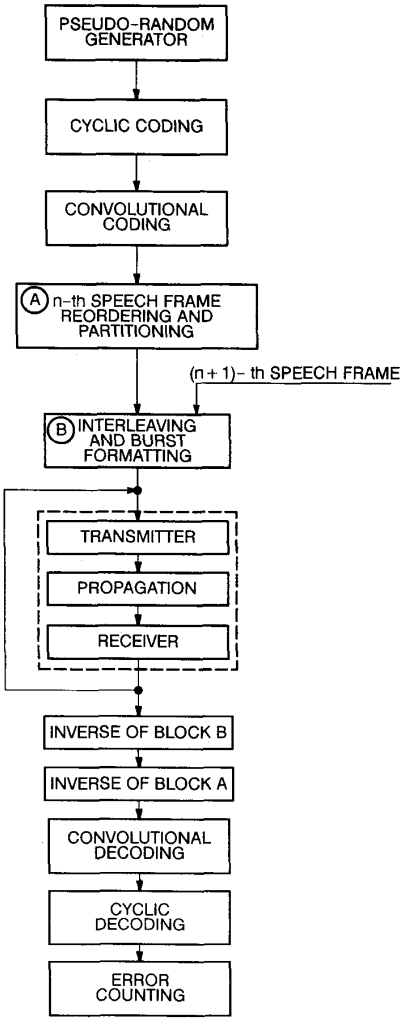

Fig. 1. Simplified flowchart of the operations performed by the software package called TDMAGSM.

the encoder receives a block of 260 information bits (speech frame) every 20 ms corresponding to a transmission rate of 13 kb/s. Since some bits of the speech frame have a greater influence on the speech quality than others, the error control is applied selectively by subdividing them into classes.

This process is illustrated in Fig. 2, according to [1]: the first 182 bits, named class 1 bits, are coded, while the other 78, named class 2 bits, are not coded. Besides, the bits of class 1 are divided in two subclasses: class 1a and class 1b. Class 1a includes 50 bits which are coded by a systematic cyclic code, adding three parity check bits in order to detect the presence of transmission errors in the output stream. The bits of class 1a plus the three added parity check bits and the 132 bits of class 1b (plus four tail bits) are reordered and convolutionally encoded. The 378 bits so obtained, joint to the uncoded 78 bits of class 2, are reordered and partitioned in eight sub-blocks before the block diagonal interleaving is applied, according to the rules indicated in [1]. Such an operation is performed

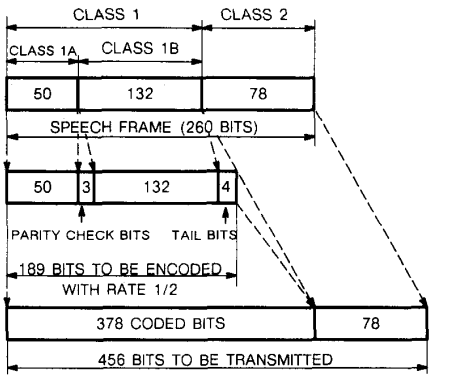

Fig. 2. Subdivision into classes and coding of the speech channel (TCH/FS).

to spread the transmission errors, tending to occur in bursts, in the radio channel. That spreading improves significantly the error correction capability of the convolutional code. After the interleaving, signal bursts like those shown in Fig. 3 are formatted.

B. Data Channel at Full Rate (TCH/F2.4)

In the case of the data channel at full rate, for services up to 2.4 kb/s, the encoder receives a block of 72 information bits (data frame) every 20 ms (Fig. 4).

Unlike the case of the speech channel described in the previous subsection, no subdivision of bits into classes is performed, but, as depicted in Fig. 4, the 72 bits of each block plus four tail bits are encoded by a convolutional code with constraint length equal to 5 and rate 1/6 [1].

After this operation, 456 bits to be transmitted are obtained. Such bits are treated as described in Section II-A, as far as interleaving, burst formatting, and simulation of the modulator are concerned.

C. Stand-Alone Dedicated Control Channel (SDCCH)

The message delivered to the encoder has a fixed size of 184 information bits, as illustrated in Fig. 5.

This block of bits is first encoded using a shortened binary cyclic Fire code [1]; it adds 40 parity check bits. The so-obtained 224 bits, plus four tail bits, are then convolutionally encoded with the same code used for the TCH/FS channel.

Subsequently, the resulting 456 bits are reordered, partitioned, interleaved and formatted with the same rules as for the traffic channels (TCH) previously described.

D. Synchronization Channel (SCH)

As shown in Fig. 6, a block of 25 information bits is coded by a cyclic code [1], which adds 10 parity check bits. The 35 bits plus four tail bits are convolutionally encoded with the same code as for the TCH/FS channel (Section II-A), thus obtaining 78 bits to be transmitted.

Unlike the cases described previously, no reordering, partitioning, and interleaving operations are performed, but the

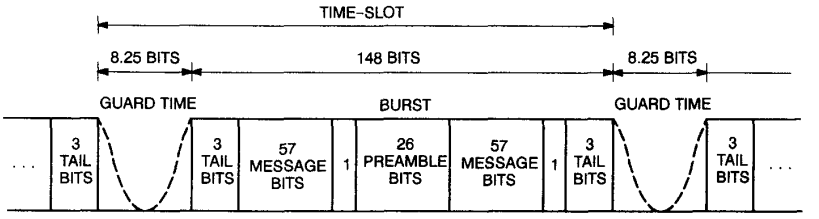

Fig. 3. Simulated time-slot structure for the TCH/FS, TCH/F2.4, and SDCCH channels. The dashed lines represent the shape of the switching transients.

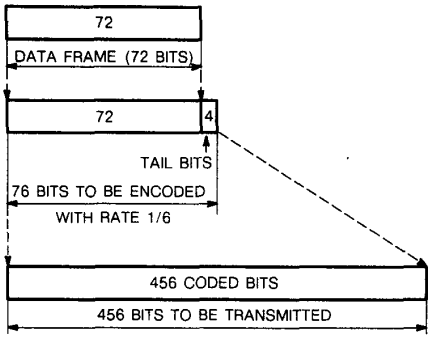

Fig. 4. Coding of the data channel (TCH/F2.4).

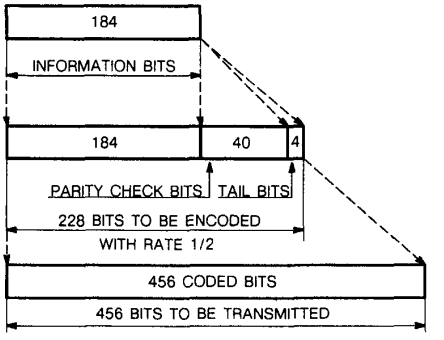

Fig. 5. Coding of the stand-alone dedicated channel.

78 bits are directly transmitted according to the burst format [1] indicated in Fig. 7.

III. Propagation Channels

The computer simulations of the propagation channel have been carried out taking into account the four following propagation conditions:

1) additive white Gaussian noise (AWGN)
2) time-varying channel (Rayleigh) with thermal noise
3) time-varying channel (Rayleigh) with interference
4) frequency-selective and time-varying channel.

A. AWGN

For the AWGN channel the BER performance is computed versus the E_b/N_0 (energy per transmitted bit/noise spectral density) ratio.

B. Time-Varying Channel with Thermal Noise

The adopted fading model simulates the attenuation with Rayleigh statistics, flat characteristics in the frequency domain and varying in the time domain. The Doppler frequency shift is included, according to the "classical model" defined in [6]. It is assumed that fadings affecting bursts belonging to different frames are uncorrelated, as would happen by using frequency hopping.

An ideal carrier phase recovery is assumed, which subtracts from the phase of the wanted signal the one due to the fading affecting it in the middle of the preamble sequence.

The BER performance is computed versus the median value of E_b/N_0, for a given value of the vehicle speed.

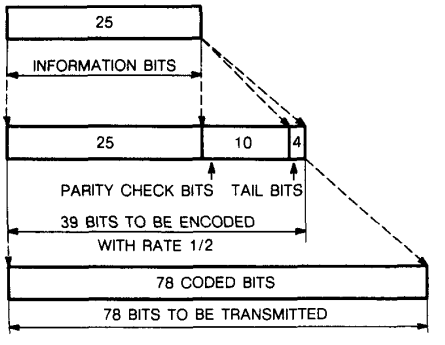

Fig. 6. Coding of the synchronization channel .

C. Time-Varying Channel with Interference

Fig. 8 shows the case of flat Rayleigh fading with interference. It is assumed that fadings affecting the wanted and the interfering signals are uncorrelated.

The BER performance is computed versus the short-term mean value of the carrier/interference (C/I) ratio for given vehicle speeds.

D. Frequency-Selective and Time-Varying Channel

The received signal usually consists of multipath components, arising from diffusion, diffraction, and scattering due to surrounding obstacles. Each multipath component can be thought of as an independent traveling plane wave, whose amplitude, phase, incoming angle and time delay are random variables. As a consequence the mobile propagation channel is

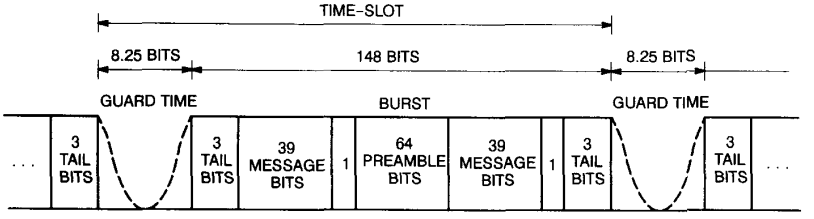

Fig. 7. Simulated time-slot structure for the SCH channel. The dashed lines represent the shape of the switching transients.

described by a random process, whose statistical characteristics are to be investigated [7]–[10]. To state the stationarity in the time (or space) domain of such a random process it can be useful to suppose the mobile channel as the result of two overlapping processes both stationary, characterized by different periodicities. The "slow" random process, usually known as "shadowing," is related to the large scale fluctuations; for example, in an urban area, it is related to the density and the average height of the buildings or the width of the streets. This process is assumed to be stationary over some hundreds of meters and the received signal is log-normally distributed [10], [11]. The short-term random process is mainly related to the motion of the mobile station through the spatial standing-wave pattern [12] resulting from the local multipath interference and is responsible for the fluctuations of the propagation channel within fractions of a wavelength. This process can be supposed stationary over some tens of wavelengths (on the order of 4–5 m, in the 900 MHz band) and with statistics of the Rayleigh type. To define the propagation model, it is assumed that the communication channel between base and mobile stations can be formally handled as a time and frequency dependent linear filter (TFLF model: time-frequency linear filter), identified by its transfer function $H(t, f)$ representative of the above-mentioned short-term random process. The time evolution of $\mathrm{Re}\{H(t, f_c)\}$ at a fixed frequency (e.g., the carrier frequency f_c) is described through a factorization formalism related to the discrete Fourier series expansion, i.e., [13]

$$\mathrm{Re}\{H(t, f_c)\} = A_0(f_c) + 2\left\{\sum_{n=1}^{N-1}[A_n(f_c)\cos(n2\pi\nu_0 t) + B_n(f_c)\sin(n2\pi\nu_0 t)]\right\} + A_N(f_c)\cos(N2\pi\nu_0 t) \quad (1)$$

where N is the number of harmonics required in order to give a satisfactory description of the time evolution, ν_0 is the fundamental harmonic of the series expansion ($1/\nu_0$ represents the time duration of the sample of $H(t, f_c)$), and $\{A_n(f_c), B_n(f_c)\}$ is a set of frequency-dependent and time-constant coefficients.

The bandwidth $N\nu_0$ in (1) is related to the well-known Doppler bandwidth, and depends on the environment and on the vehicle speed. The coefficient set $\{A_n(f_c), B_n(f_c)\}$ determines the shape of the Doppler spectrum at a given f_c and depends on the distribution of angles of incidence of the incoming multipath components at the mobile station [9],

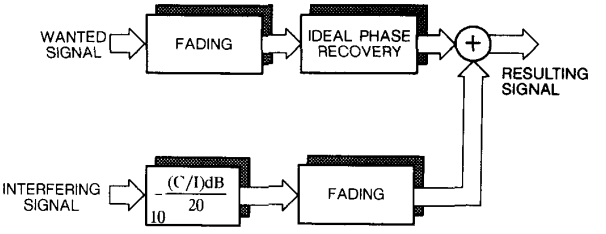

Fig. 8. Simplified block diagram of the time-selective channel with interference.

[14]. The fine characterization of the channel transfer function within a given frequency band requires the knowledge of a sufficient number of sets $\{A_n(f_c), B_n(f_c)\}$. The number ensuring a satisfactory discrete description of the propagation model depends on the transmitted signal bandwidth and on the dynamic properties of the transfer function, i.e., on the rapidity of the transfer function fluctuations versus frequency.

To properly describe the frequency characteristics of the mobile propagation channel in the modulation bandwidth, the discrete Fourier series expansion of the real part of the instantaneous (i.e., at $t = t_0$) transfer function is used:

$$\mathrm{Re}\{H(t_0, f)\} = \mathcal{A}_0(t_0) + 2\left\{\sum_{m=1}^{M-1}[\mathcal{A}_m(t_0)\cos(m2\pi\tau_0 f) + \mathcal{B}_m(t_0)\sin(m2\pi\tau_0 f)]\right\} + \mathcal{A}_M(t_0)\cos(M2\pi\tau_0 f). \quad (2)$$

In this case τ runs in the echo time delay domain.

As is known, the time delay spectrum determines the frequency selectivity of the channel and plays a role similar to that of the Doppler spectrum in determining the time selectivity. According to such an interpretation, in (2) $F = 1/\tau_0$ is the bandwidth in which the proper description of the frequency-selectivity effects is restricted, whereas $M\tau_0$ is the maximum delay corresponding to the environment under examination.

The coefficient set $\{\mathcal{A}_m(t_0), \mathcal{B}_m(t_0)\}$ determines the shape of the instantaneous delay spectrum. As before, in order to know the time evolution characterization of the transfer function with a proper time resolution, knowledge of a sufficient number of sets is required.

As regards the coefficient sets in (1) and (2), to make the model handling easier without loss of accuracy, two

stationarity hypotheses can be made:

$$\left[A_n^2(f) + B_n^2(f)\right]_{f_s f_s} = |S_n|^2 \quad \text{(3a)}$$

$$\left[\mathcal{A}_m^2(t) + \mathcal{B}_m^2(t)\right]_{t_s t_s} = |T_n|^2. \quad \text{(3b)}$$

Hypothesis (3a) implies that the Doppler effect is frequency-independent in the stationary band f_s. Hypothesis (3b) implies that the time-delay profile is time-independent during the stationary period t_s.

The TFLF model outlined above shows its advantages in the $H(t, f)$ simulation and calibration procedures, which have to take account of the physical values obtained by measurements.

1) Software Simulation: The study of time evolution, for a fixed frequency f_c, of a mobile channel requires the knowledge of the Doppler power spectral density of the real and imaginary parts of $H(t, f_c)$. To this purpose, a parabolic shape $|S_n|^2$ is assumed to represent the Doppler spectrum in the Doppler band. Out of this band the Doppler spectrum is assumed to be zero.

The simulation process basically consists of two parallel and independent computational flows, one for $\mathrm{Re}\{H(t, f_c)\}$ and the other for $\mathrm{Im}\{H(t, f_c)\}$. Starting from the shape $|S_n|^2$, and simulating spectral amplitudes with uniformly distributed phases, the complex quantity S_n is evaluated (coefficient set $\{A_n(f_c), B_n(f_c)\}$). Assuming the real and imaginary part to be even and odd, respectively, the complex quantity S_n can be interpreted as the Fourier transform of a real signal. Two independent inverse Fourier transforms, numerically performed by a FFT technique, give the time realization of the real and imaginary parts of the channel transfer function relative to an urban multipath environment. A different environment, such as a suburban or rural area, can be simulated by adding a deterministic component to the transfer function simulated as described above. Such a deterministic component stands for the main and constant propagation path, characterized by a power ρ, relative to that of the random multipath component.

For low values of ρ ($\sim$0 dB) random contributions prevail, which reflect into a Rayleigh distribution for $|H(t, f_c)|$; it can be shown that even a moderate increase of ρ (from 5 to 10 dB) causes remarkable changes in both statistical and dynamic properties of the transfer function.

On the basis of a qualitative interpretation of some experimental results [10], [11] the following classification is drawn:

a) Urban center—high building density (>30%): $\rho = -\infty$ (dB) (only multipath component)
b) Urban area—moderate building density (20%–30%): $\rho = 0$ to 4 (dB)
c) Urban area—low building density (10%–20%): $\rho = 4$ to 6 (dB)
d) Suburban area: $\rho = 6$ to 10 (dB)
e) Open (or rural) area: $\rho > 10$ (dB).

In Fig. 9 the spectral power densities of $\mathrm{Re}\{H(t, f_c)\}$ (or $\mathrm{Im}\{H(t, f_c)\}$) are reported, obtained by averaging 300 simulated realizations (for each value of ρ). In the curve (a) ($\rho = -\infty$ dB) only the random multipath channel is present, whereas the other curves experience the effects of the increasing of the deterministic component.

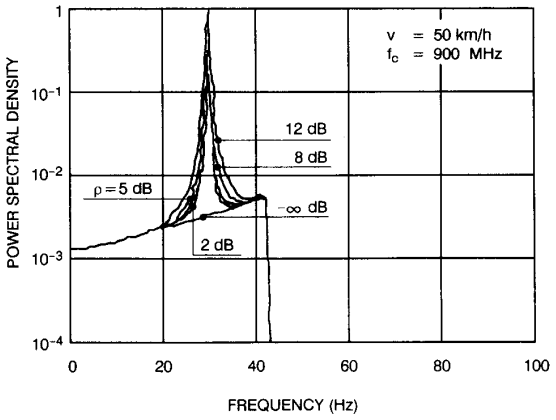

Fig. 9. Average simulated spectra of $\{H(t, f_c)\}$ (or $\mathrm{Im}\{H(t, f_c)\}$).

As far as frequency-selective characteristics are concerned, we start from the delay profile of the incoming echoes, i.e., the impulse response of the TFLF, representative of the short-term propagation characteristics. Also in this case, two independent and parallel branches are simulated in order to compute $\mathrm{Re}\{H(t_0, f)\}$ and $\mathrm{Im}\{H(t_0, f)\}$ starting from their delay spectra, respectively.

The first simulation step deals with the power spectral density $|T_m|^2$ of delays; a generic simulation of phases, assumed uniformly distributed in the range $[-\pi, \pi]$, leads to the complex form of T_m (i.e., the coefficient set $\{\mathcal{A}_m(t_0), \mathcal{B}_m(t_0)\}$). Introducing the usual symmetry assumption, the Fourier transform of a real signal is obtained. The inverse Fourier transform gives $\mathrm{Re}\{H(t_0, f)\}$ as a function of frequency. Similarly, the other simulation branch furnishes $\mathrm{Im}\{H(t_0, f)\}$.

The so-obtained transfer function $H(t_0, f)$ is a single realization of the random process characterized by the delay spectrum $|T_m|^2$, and depends on the considered environment and on f_c.

Finally, a satisfactory relationship between the environment and $|T_m|^2$ remains to be faced. Unfortunately, most available experimental results have been obtained using an impulse technique and provide the amplitude delay profiles (i.e., the delay profiles of $|H(t_0, f)|$): no information about the phase (or about both the real and the imaginary parts of the transfer function) is usually available.

The method used hereafter is based on an iterative procedure that provides, by successive approximations, the spectral profiles $|T_m|^2$ of $\mathrm{Re}\{H(t_0, f)\}$ and $\mathrm{Im}\{H(t_0, f)\}$ (corresponding to measured or proposed delay profiles of $|H(t_0, f)|$) to be used as inputs to the simulation process.

An example of the calibration of the model, obtained by using the above-mentioned iterative method, is shown in Fig. 10. The dashed line (a) is the ETSI/GSM [6] proposed spectrum time delay profile of $|H(t_0, f)|$ for a 900 MHz urban and suburban mobile channel.

The curve (b) represents the spectral profile $|T_m|^2$ of $\mathrm{Re}\{H(t_0, f)\}$ (or $\mathrm{Im}\{H(t_0, f)\}$) and is characterized by an

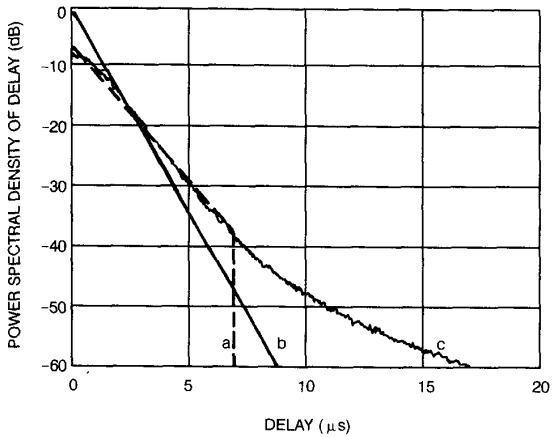

Fig. 10. Delay profiles of modulus and real (or imaginary) part of $H(t_0, f)$.

exponentially decreasing behavior (mean value and standard deviation equal to 0.65 μs).

The mean spectral profile of $|H(t_0, f)|$ is then computed by averaging 300 independently simulated profiles. The result is reported as (c) in Fig. 10. It is worth noting that (c) well fits (a). Then the spectrum profile (b) used in our simulation model can stand for the urban and suburban propagation channel proposed by ETSI/GSM (notice that the portion of spectrum beyond 7 μs is practically negligible, because of its poor power content).

The above-outlined simulated model provides separate time-domain $(H(t, f_c))$ and frequency-domain $(H(t_0, f))$ realizations of $H(t, f)$.

In [13] a bidimensional realization of the transfer function $H(t, f)$ is obtained in order to simulate a wide-band (frequency-selective) dynamic channel.

Figs. 11(a) and 11(b) show two examples of bidimensional simulation as far as the envelope of the transfer function is concerned, for the typical urban and hilly areas, according to the delay profile definition of ETSI/GSM [6] (see Fig. 10 for the typical urban case); the mobile speed is 50 km/h. The whole simulations of Figs. 11(a) and 11(b) cover a bandwidth of about 8 MHz and last about 100 ms. The plots are relevant to an interesting segment limited to a 300 kHz bandwidth (centered around f_c); the time resolution is $5 \cdot 10^{-5}$ s (within this period of time the channel transfer function is meant to be constant).

IV. Receiver Characteristics

A. IF and BB Filtering Characteristics

With reference to the receiver block diagram of Fig. 12, the receive filtering has been optimized for the best performance [15], and consists of two cascaded Butterworth filters, both ideally equalized, the first with seven poles and 3 dB bandwidth equal to 25/16 the bit rate, the second with five poles and 3 dB bandwidth equal to half the bit rate.

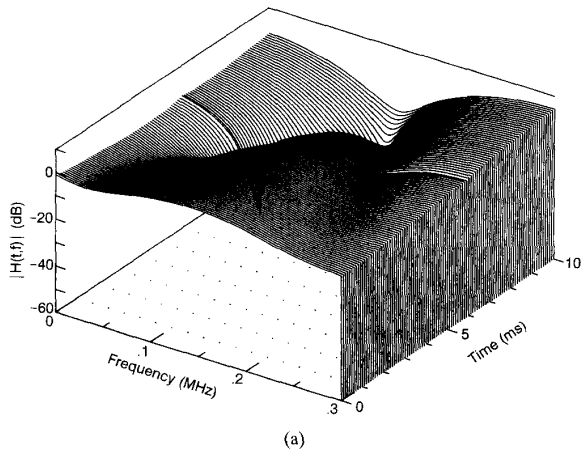

(a)

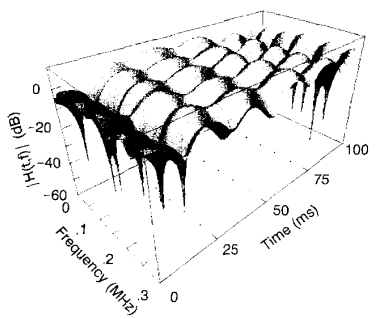

(b)

Fig. 11. Example of simulation of $|H(t, f)|$ in the case of propagation in typical urban area. (b) Example of simulation of $|H(t, f)|$ in the case of propagation in hilly area.

B. Synchronization and Channel Impulse Response Estimation

To recover the necessary symbol timing and carrier phase of the coherent GSM receiver, the correlation properties of suitably designed [4] binary sequences are exploited.

In particular, eight different synchronization sequences ("midambles") have been defined [16], with good cross-correlation properties in order to reduce the effects of interference among transmitters operating at the same frequency: the sequence used in this work is 00100101110000100010010111; notice that only the central 16 bits have been selected for suitable correlation properties, while the first and last five bits have been added to account for the time dispersion of the channel impulse response and the time-jitter of the received signal burst.

The synchronization strategy adopted in this paper first oversamples (e.g., four samples/symbol) the received 26–bit midamble sequence (this is performed by the sampling processor of Fig. 13). Such an oversampling produces K (e.g., $K = 4$ in the case of 4 samples/symbol) received midamble sequences $r_i(t), i = 1, \cdots, K$.

Second, K complex correlation functions $R_i(t), i = 1, \cdots, K$ between the corresponding sequences $r_i(t)$ and the midamble reference complex sequence are computed. The reference complex midamble $v(t)$ stored in the receiver (ROM of

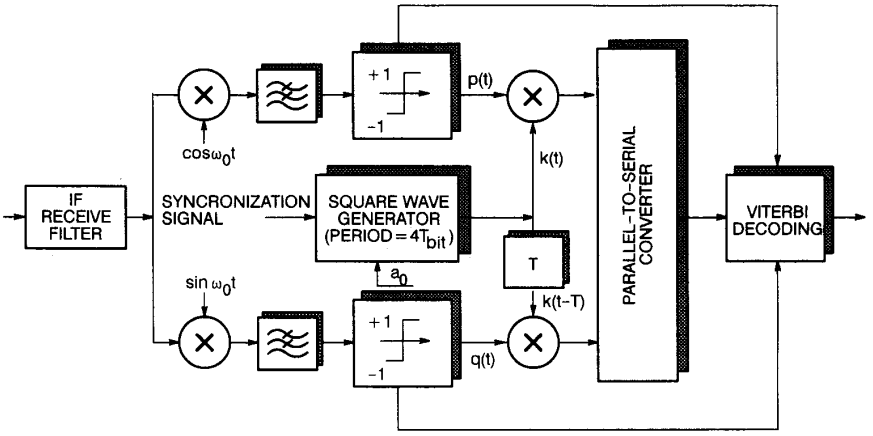

Fig. 12. Simplified block diagram of the simulated receiver.

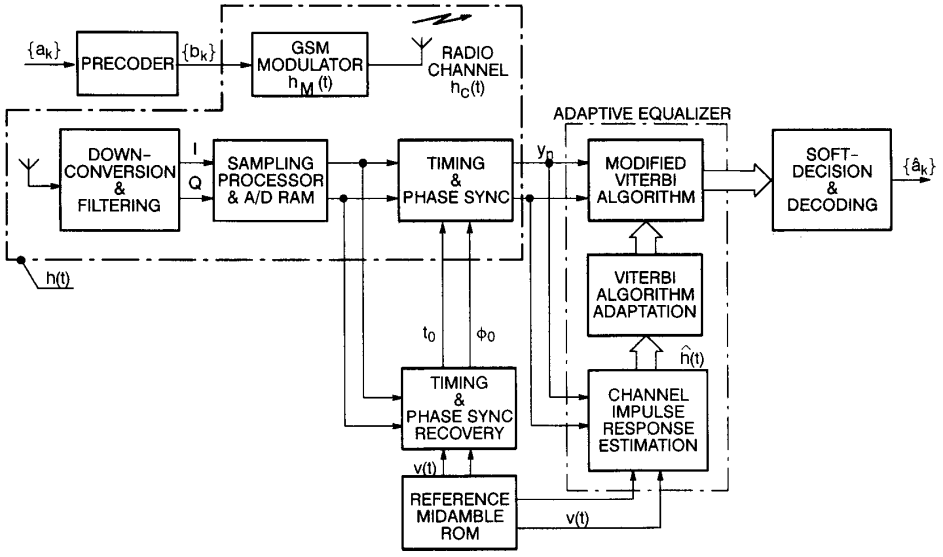

Fig. 13. Block diagram of the simulated ETSI/GSM system.

Fig. 13) has been obtained by sampling the 16 central symbols of a 26-symbol MSK-modulated signal; the modulating sequence is formed by the precoded symbols $\{b_k\}$ of Fig. 13. Of course the in-phase and quadrature components of the so-obtained reference complex midamble are offset by a bit period T.

The K magnitudes $A_i(t), i = 1, \cdots, K$ of the correlation functions $R_i(t)$ are then given by

$$A_i(t) = \sqrt{\left[R_i^I(t)\right]^2 + \left[R_i^Q(t)\right]^2} \tag{3}$$

where $R_i^I(t)$ and $R_i^Q(t)$are the in-phase and quadrature components of $R_i(t)$, respectively.

Third, the sampling instant t_0 is obtained as the peak instant of that $A_i(t)$ with maximum peak value, with a further time shift of $(j-1)T/K$, which takes account of oversampling; j is the value of index i corresponding to that $A_i(t)$ with maximum peak value.

Fourth, the carrier phase reference ϕ_0 is identified as

$$\phi_0 = \arctan \frac{R_j^Q(t_0)}{R_j^I(t_0)}. \tag{4}$$

The computation of the channel impulse response $h(t)$ necessary to the Viterbi adaptive equalizer, as discussed in what follows, is performed by using the complex correlation $R_{xv}(t)$ between $v(t)$ and the 26 samples of the received and synchronized midamble $x(t)$. As shown in [4], it is $R_{xv}(t) = R_{vv}(t) \star h(t)$, with the auto-correlation function $R_{vv}(t)$ of $v(t)$ equivalent to a delta function within the neighborhood of ± 4 bits around its central value.

In the case of a 16-state Viterbi adaptive equalizer, as the one used in this paper, only five consecutive samples of $h(t)$,

alternately real and imaginary, namely

$$h(t) = \sum_{i=-1}^{1} h^I_{-2i}(t_0 - 2iT) \cdot \delta(t - 2iT) + j \sum_{i=0}^{1} h^Q_{-2i+i}[t_0 - (2i+1)T] \cdot \delta[t - (2i+1)T] \tag{5}$$

have to be considered and passed to the equalizer. To do this, an "energy window" of five symbol periods is slid along $h(t)$ to search for the sequence of five samples with maximum energy.

C. Demodulation and Regeneration

The used demodulation is of coherent type. Thanks to the precoding of the modulating bit stream included in the GSM modulation [5], after the coherent demodulator the sampled data values $p(t)$ and $q(t)$ multiplied by a sign inversion function $k(t)$, opposite on the two branches (see Fig. 12), are uncorrelated and the modulation process is practically equivalent to that of an offset-4PSK.

D. Viterbi Adaptive Equalizer

This kind of equalizer does not, in the strict sense, attempt to equalize the channel impulse response. Rather, it uses the knowledge of the channel impulse response (through an estimation technique) and of the received signal in order to find the most likely transmitted data sequence. Its performance is therefore dependent on the available estimate of the channel impulse response as well as on the symbol timing and carrier phase recovery, as discussed before.

It is well known that in a maximum likelihood sequence estimation [17], [18], a metric is required to discriminate among all the possible transmitted sequences: the most likely sequence is that which maximizes the likelihood function [17], [18].

In general, computation of the likelihood function requires passing the received signal through a matched filter with impulse response $h^*(-t)$ followed by a processing of the sampled outputs of the matched filter. A brute force approach of computing the value of the likelihood function for each of the possible data sequences would be very inefficient. Instead, the Viterbi algorithm reduces the computational burden by observing that the incremental metric at time instant $k = n$ depends only on the sequence

$$\alpha^m_n, \alpha^m_{n-1}, \cdots, \alpha^m_{n-L}$$

where α_k are, in the case of the ETSI/GSM radio signal, alternately real and imaginary, L is the number of significant interfering samples of $h(t)$, m denotes the generic mth sequence.

Further simplifications to the incremental metric computation can still be made for GMSK by observing that $\alpha_k = \pm 1$ or $\pm j$ and by noting that at $k = n$ either the real or the imaginary part of the signal y_n of Fig. 13 is needed, but not both. Hence, the matched filter implementation can be somewhat simplified. Finally, a term of the incremental metric can only have 2^{L+2} possible values, and hence these can be stored in a look-up table prior to the Viterbi algorithm operation, to be recalled when required. In practice, in this paper we have computed the incremental metric $\wedge_{mn}$ through the following formula

$$\wedge_{mn} = \wedge_{m(n-1)} + \mathrm{Re}\{(\alpha^m_n)^* \cdot (y_n - P_s)\} \tag{6}$$

where P_s is a complex number read from a look-up table corresponding to the state s for which a survivor is being searched.

To perform the demodulation of the received signal burst, the Viterbi adaptive equalizer starts its operation from the information bits close to the midamble, which should undergo similar channel distortions, and works rightward and leftward (the received time slot is completely stored before starting its processing).

The Viterbi equalizer described above is derived from the idea first proposed in [19], and was adopted in [4], [20]. It requires only four additions per state and does not require any noise whitening because it operates on the sampled outputs of the matched filter.

In this paper we have further simplified the equalizer scheme by using a fixed filter rather than a matched filter, always without noise whitening (Fig. 13). Since such a filter already exists in the bandpass filter of the receiver described above, no processing is essentially required apart from signal sampling before the Viterbi algorithm. This kind of receiver can be considered to be matched to the average channel, and degradation due to noise enhancement will appear if the channel transfer function shows notches near the carrier frequency. On the other hand, the absence of a matched filter will increase the sensitivity of the receiver to initial timing [18].

E. Viterbi-Algorithm Decoding

After regeneration, the digital stream undergoes the inverse operations of interleaving, partitioning, and reordering described in Section II.

The convolutionally encoded bits are then decoded by a 16-state Viterbi algorithm.

The Viterbi algorithm can be applied either with soft-decision or with hard-decision [17], [18], [20], according to the way the metric is computed, i.e., in the first case exploiting the Euclidean distance between the regenerated code-words and all the possible words of the code, in the second evaluating the simpler Hamming distance.

Soft-decision turns out to be more effective than hard-decision, as it carries, for each regenerated bit, information about its "degree of reliability." In this work, the "degree of reliability" is obtained considering the amplitude of the received signal at the sampling instants. In particular, this is done by applying at the regeneration stage (see Section IV-C), a limiting function to each signal sample, according to the characteristic shown in Fig. 14. After that the sample is quantized and, at each step, the metric is updated by adding to its current value the absolute value of the difference between the limited and quantized signal sample and the nominal value the sample should have.

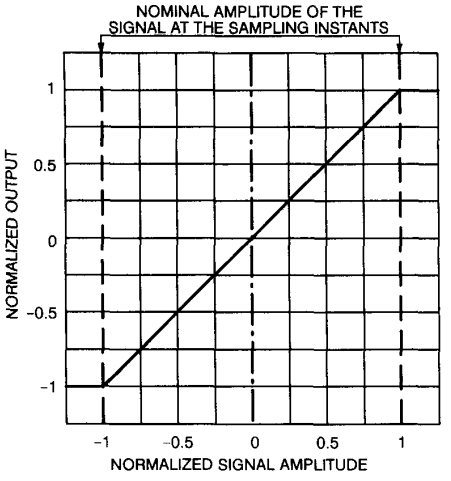

Fig. 14. Limiting characteristic used in the metric computation of the soft-decision Viterbi algorithm.

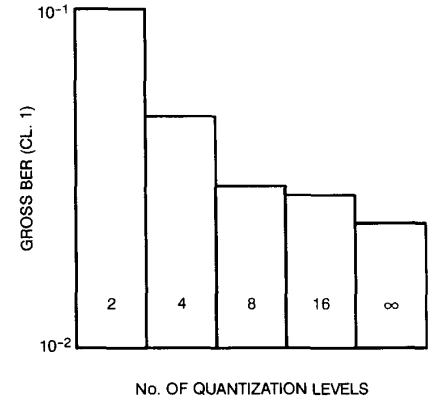

Fig. 15. Gross BER (class 1) in the case of speech channel with the use of frequency hopping (mobile speed $\simeq$ 0 km/h, C/I = 5 dB) versus the number of quantization levels of the signal components. Channel: TCH/FS.

If the quantization is performed on two levels, the soft-decision technique works just as the hard-decision, whereas increasing the number of quantization levels makes the information associated with it more accurate, but increases the implementation complexity.

In Fig. 15 some results relevant to TCH/FS (see Section II-A) are reported to investigate the performance of the adopted soft-decision versus the number of quantization levels of the signal at the output of the limiting device. The performance has been calculated by simulating the propagation channel described in Section III-C, in the case of C/I ratio equal to 5 dB and mobile speed near 0 km/h. The presented results, reported for the sake of conciseness just for the Gross BER's (defined in Section V-A) of class 1 bits, highlight that a good trade-off between the number of quantization levels and the achievable performance can be obtained with only 8 quantization levels. It has been verified that this conclusion can be considered valid in general.

As an example of the gain achievable with soft-decision technique, for the simulated speech channel at full rate and in the case of a Rayleigh fading channel with interference, with the usage of frequency hopping and for a mobile speed tending to 0, a residual BER (see next section) of 10^{-2} is obtained at C/I = 7.6 dB with hard-decision, and at C/I = 4.5 dB with soft-decision (without coding more than 15 dB would be necessary). At 300 km/h the corresponding values are 9.6 and 5.4 dB (without coding an irreducible BER greater than 10^{-2} arises).

V. Performance Results

A. TCH/FS Channel

For the speech channel at full rate the parity check bits (see Section II-A) are exploited to update a flag indicating whether the error correction has been successful or not, or, in other words, whether a frame has to be considered "good" or "bad."

Then, the error counting is performed over the classes of bits 1a, 1b, 1, 2, defined in Section II-A, evaluating the following quantities:

- Gross BER (ratio of the number of errors detected over all the transmitted frames to the total number of transmitted bits);
- BFI ratio (bad frame indication, ratio of the number of frames defined as "bad" to the total number of transmitted frames);
- Residual BER (ratio of the number of detected errors in the "good" frames to the number of transmitted bits in the "good" frames).

According to the above definition of residual BER, an indetermination may arise if no good frames occur in the averaging interval; in this case it is assumed that the Residual BER takes the values 0.5 by default.

It is worth noting that the curves corresponding to class 2 bits can be taken as the reference curves without coding.

1) Results in AWGN and Time-Varying Channel: Figs. 16 and 17 refer to the case of AWGN channel and the case of time-varying channel with thermal noise for a mobile speed of 50 km/h. In particular, Fig. 16 pertains to the BFI ratio while Fig. 17 pertains to the residual BER; for the sake of brevity no results of gross BER are presented. In AWGN channel a residual BER of 10^{-2} is obtained at E_b/N_0 equal to -0.9 dB for "class 1" bits, and at $E_b/N_0 = 4.8$ dB for the uncoded bits "class 2." The same residual BER is obtained in a time-varying channel with thermal noise at median value of $E_b/N_0 = 2.6$ dB for "class 1" bits, and at 14.2 dB for the uncoded bits ("class 2").

2) Results in Time-Varying Channel with Interference: Figs. 18 and 19 pertain to the case of varying channel with interference for mobile speeds near 0 and at 300 km/h, respectively.

For mobile speed of about 0 km/h the residual BER of 10^{-2} is obtained at C/I equal to 4.5 dB for "class 1" bits, while without coding more than 15 dB would be necessary. If the mobile speed increases up to 300 km/h, a worsening of about 1 dB at BER = 10^{-2} in the case of the coded bits

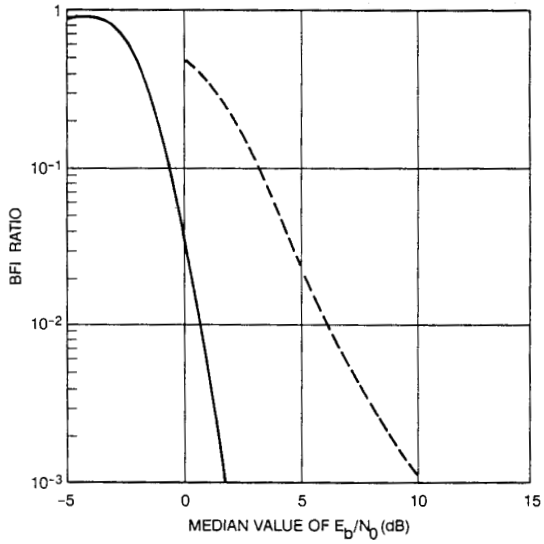

Fig. 16. BFI ratio versus E_b/N_0 (energy per transmitted bit/noise spectral density) in AWGN (continuous line) and in a time-selective channel with thermal noise for a speed of the mobile unit of 50 km/h (dashed line). Simulated GSM channel: speech channel (TCH/FS).

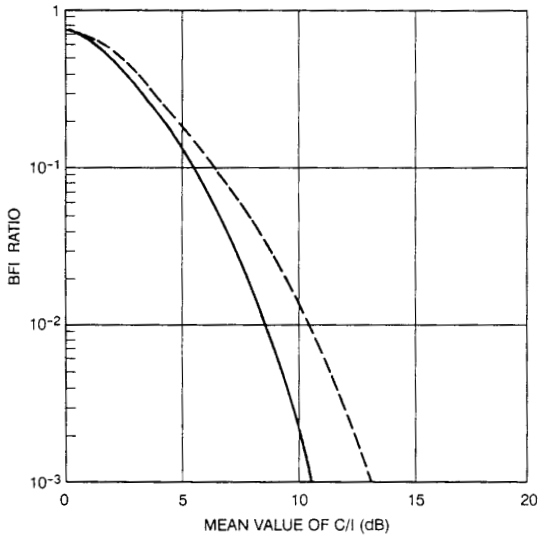

Fig. 18. BFI ratio versus C/I in a time selective channel with interference (no thermal noise) for vehicle speeds of about 0 km/h (continuous line) and 300 km/h (dashed line). Simulated GSM channel: speech channel (TCH/FS)

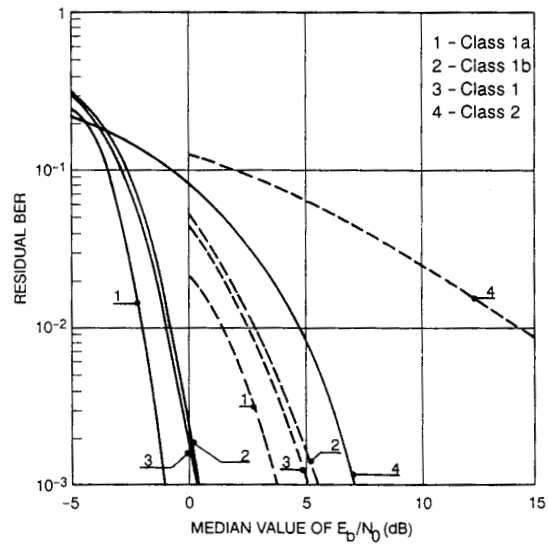

Fig. 17. Same as Fig. 16 but for residual BER.

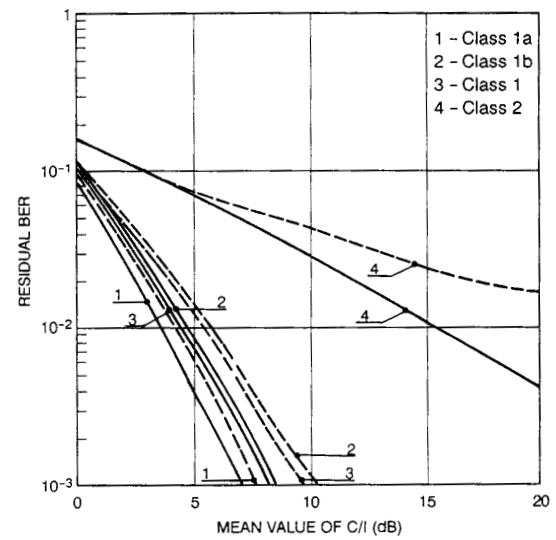

Fig. 19. Same as Fig. 18 but for residual BER.

has been found, while without coding the performance curve presents an asymptotic irreducible BER just above 10^{-2}.

3) Results in Frequency and Time-Varying Channel: In this case, the adaptive equalizer is effective to reduce the frequency-selective distortions.

The Viterbi equalizer described above is initialized through a channel impulse response estimation, together with symbol timing and carrier phase recovery, during the midamble transmission period, at the center of the basic time slot of Fig. 3. Then no tracking of the changes in the channel response over the two information data transmission periods is performed. However, the positioning of the reference sequence in the middle of the slot leads to a total delay of about 250 μs only between channel estimation and the last information bit on either side, thereby reducing the effects of the channel characteristic variations at a given vehicle speed.

The changes in the channel response are simulated through the propagation characteristic modeling technique outlined in the previous sections, which provides a set of time- and frequency-dependent linear filters (TFLF's) $\{H_i(t,f)\}, i = 1, \cdots, M$.

Of course, the number of $H_i(t,f)$ affecting a given time slot depends on the vehicle speed v. For example, when

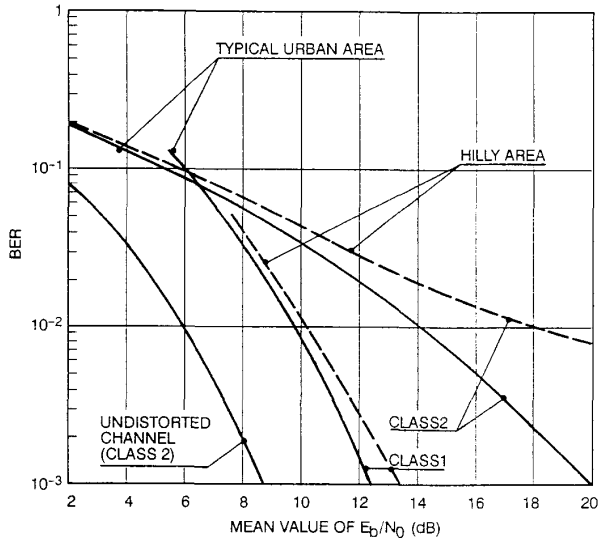

Fig. 20. Bit error rate of the ETSI/GSM system with a 16-state Viterbi equalizer, in the case of typical urban and hilly propagation models.

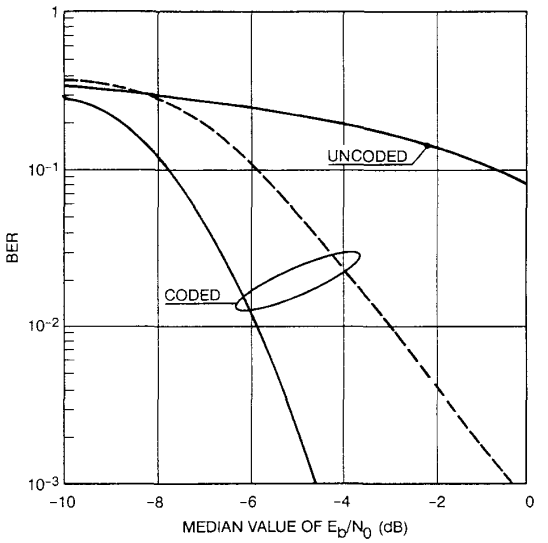

Fig. 21. BER performance versus E_b/N_0 in AWGN (continuous line) and in a time selective channel with thermal noise for a speed of the mobile unit of 50 km/h (dashed line). Simulated GSM channel: data channel (TCH/F2.4)

$v = 50$ km/h eleven different $H_i(t, f)$ have to be considered per each time slot. This means that each $H_i(t, f)$ "covers" $156.25/11 = 14.2$ bits, during which the channel transfer function is meant to be constant.

Consequently, the Viterbi equalizer is initialized according to the channel characteristics corresponding to the central filters $H_i(t, f)$, but it will have to equalize the channel distortions corresponding to the preceding $H_i(t, f)$ (leftward operation) and to the following $H_i(t, f)$ (rightward operation). The same is repeated in the following time slots, by considering different sets of eleven $H_i(t, f)$. The higher the vehicle speed, the greater the equalizer mismatching.

Moreover, since we have to adopt the block diagonal interleaving with depth 8, as specified in [1], the sets of consecutive filters $H_i(t, f)$ are drawn from $\{H_i(t, f)\}, i = 1, \cdots, M$ with the same time periodicity.

Our simulation program, which is frequency-domain based, builds the distorted bit sequence of the basic time slot by performing eleven (in the case of $v = 50$ km/h) filterings of the modulated signal through eleven $H_i(t, f)$ and by joining the pertaining 14.2 bits in the right order. This operation has to be repeated for a number of times large enough to get the required statistical completeness.

BER results of the above described Viterbi equalizer are given in Fig. 20 for $v = 50$ km/h and for the two cases of typical urban and hilly areas. In particular, the BER curves for the distorted channels are relevant to the uncoded class 2 bits, and to the coded bits of classes 1a and 1b. In the latter case only the hard-decision technique has been considered.

B. TCH/F2.4 Channel

For the data channel TCH/F2.4 the error counting is performed by evaluating the BER as the ratio of number of detected errors to total number of transmitted bits.

The performance results are gathered in Figs. 21 and 22 for three out of the four considered propagation conditions, i.e., AWGN channel, time-varying channel with thermal noise, and time-varying channel with interference. From the reported results it is worth noting that the considered convolutional code with high redundancy (rate 1/6) allows substantial gains to be obtained. For example, in a time-varying channel with interference the coding gain at BER $= 10^{-2}$ is about 15.9 dB. Furthermore, we have found that with the considered coding the difference between the cases of vehicle speeds near 0 (with frequency hopping) and at 300 km/h is negligible at BER greater than 10^{-3}.

C. SDCCH and SCH Channels

As in the case of speech channel, also in these channels the parity check bits are used to set a flag indicating whether the regenerated frame has to be considered "good" or "bad."

As a consequence, the performance is evaluated in terms of BFI ratio and gross and residual BER, according to the same definitions given in Section V-A.

The performance results are depicted in Figs. 23 and 24 for the SDCCH channel and in Figs. 25 and 26 for the SCH channel.

In both channels only the BFI ratios are reported because during our computer simulations (carried out for a maximum of four hundred thousand information bits), no errors have been detected in the "good" frames. This result is a consequence of the high number of parity check bits added by the considered cyclic codes.

Finally, it is worth noting that for the two simulated GSM control channels (SDCCH and SCH) the simple concept of the bad frame indication defined in Section V-A, exploiting the high number of parity check bits added by the considered cyclic codings (40 and 10 for SDCCH and SCH, respectively),

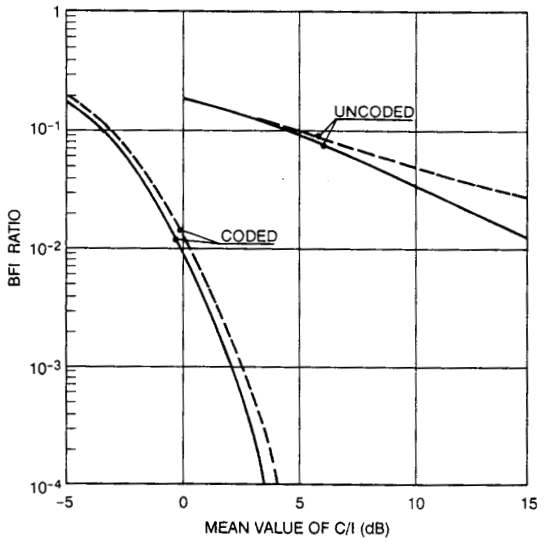

Fig. 22. BER performance versus C/I in a time-selective channel with interference (no thermal noise) for vehicle speeds of about 0 km/h (continuous line) and 300 km/h (dashed line). Simulated GSM channel: data channel (TCH/F2.4)

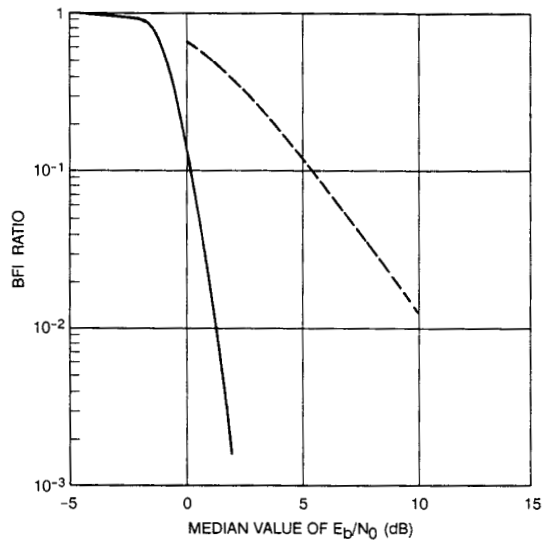

Fig. 23. Same as Fig. 16 but for the stand-alone dedicated control channel (SDCCH).

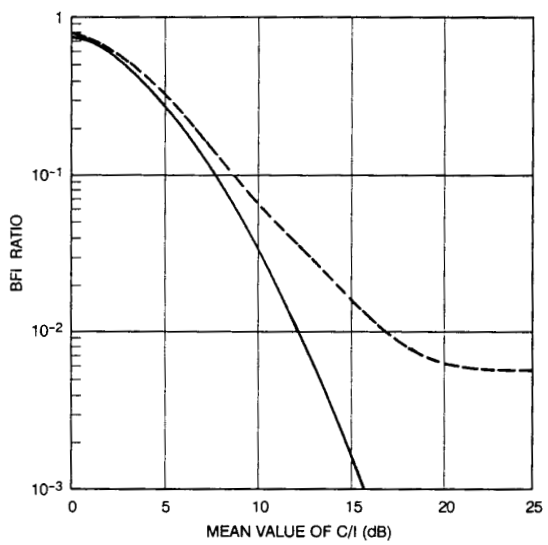

Fig. 24. Same as Fig. 18 but for the stand-alone dedicated control channel.

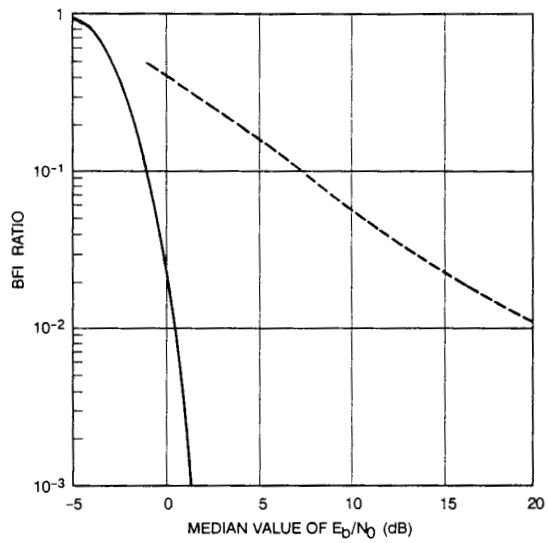

Fig. 25. Same as Fig. 16 but for the synchronization channel.

yields a very low probability of considering a regenerated frame as a "good" frame when, actually, it should be marked as a "bad" frame. Therefore, a further complication of the BFI concept, such as channel-state estimation does not seem necessary in this case.

VI. Conclusion

The computer simulation results presented show that a soft-decision Viterbi algorithm allows the performance of some ETSI/GSM traffic and control channels to be considerably improved with respect to hard-decision. This improvement can be achieved with a not too heavy increase of hardware complexity: in fact, quantizing the signal samples on 16 levels (using four bits) yields a performance very close to that given by infinite precision representation, and reducing the quantization to eight levels seems to be acceptable.

Concerning the typical urban and hilly areas defined by ETSI/GSM, the propagation modeling technique herewith presented allows realistic and efficient computer simulations.

As regards adaptive equalization, an MLSE based on the Viterbi algorithm with 16 states, which has a reasonable complexity, and without adaptation during each channel time-slot has been considered and its operation in the above-mentioned propagation environments has been studied by means of computer simulations.

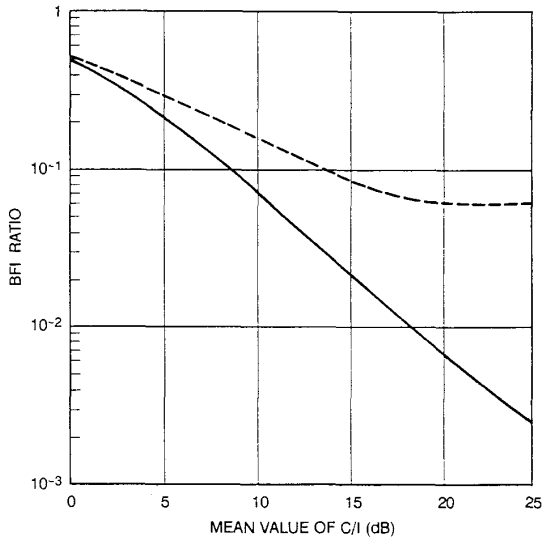

Fig. 26. Same as Fig. 18 but for the synchronization channel.

Finally, the use of adaptive equalization and soft-decision techniques has been proven to be effective when applied to the radio environment foreseen for the ETSI/GSM system.

ACKNOWLEDGMENT

The authors wish to thank Mr. L. Bassis and Mr. M. Ercolin for their contribution in the achievement of simulation results reported in this work. The authors are also grateful to Dr. L. Stola and Dr. V. Zingarelli for their valuable contribution and advice in the development of the propagation modeling and in the study and simulation of the adaptive equalization techniques, respectively.

REFERENCES

[1] GSM Recommendation 05.03, "Channel coding."
[2] F. Muratore and V. Palestini, "A computer simulation program for TDMA systems," in *Proc. Int. Conf. Digital Land Mobile Radio Commun.* Venice, Italy, July 1987, pp. 290–299.
[3] ——, "Performance of a narrowband TDMA mobile radio system with the GSM assumptions," in *Proc. Third Nordic Seminar on Digital Land Mobile Radio Commun.,* Copenhagen, Denmark, Sept. 13–15, 1988.
[4] G. D'Aria and V. Zingarelli, "Design and performance of synchronization techniques and Viterbi adaptive equalizers for narrowband TDMA mobile radio," in *Proc. Third Nordic Seminar on Digital Land Mobile Radio Commun.,* Copenhagen, Denmark, Sept. 13–15, 1988.
[5] GSM Recommendation 05.04, "Modulation."
[6] Final report of COST 207, "Digital land mobile radio communications," publication of the Commission of the European Communities, 1989.
[7] R. H. Clarke, "A statistical theory of mobile-radio reception," *Bell Syst. Tech. J.,* vol. 47, pp. 957–1000, July-Aug. 1968.
[8] W. C. Jakes, Jr., *Microwave Mobile Communication.* New York: Wiley, 1974.
[9] W. C. Y. Lee, *Mobile Communication Engineering.* New York: McGraw-Hill, 1982.
[10] Y. Okumura, E. Ohmori, T. Kawano, and K. Fukuda, "Field strength and its variability in VHF and UHF land-mobile radio service," *Rev. Elec. Comm. Lab.,* vol. 16, no. 9–10, pp. 825–873, 1968.
[11] M. F. Ibrahim and J. D. Parsons, "Signal strength prediction in built-up areas; Part 1: Median signal strength," *Inst. Elec. Eng. Proc.,* pt. F, vol. 130, no. 5, pp. 377–384, 1983.
[12] J. F. Ossanna, Jr., "A model for mobile radio fading due to building reflections: theoretical and experimental fading waveform power spectra," *Bell Syst. Tech. J.,* vol. 43, no. 11, pp. 2935–2971, 1964.
[13] G. D'Aria, L. Stola, and V. Zingarelli, "Modeling and simulation of the propagation characteristics of the 900 MHz narrowband-TDMA CEPT/GSM mobile radio," in *Proc. 39th IEEE Veh. Technol. Conf.,* San Francisco, CA, April 29–May 3, 1989, pp. 631–639.
[14] S. O. Rice, "Statistical properties of a sine wave plus random noise," *Bell Syst. Tech. J.,* vol. 27, no. 1, pp. 109–157, 1948.
[15] F. Muratore and V. Palestini, "Features and performance of 12PM3 modulation methods for digital land mobile radio," *IEEE J. Select. Areas Commun.,* vol. SAC-5, pp. 906–914, June 1987.
[16] ETSI/GSM Rec. 05.02.
[17] S. Benedetto, E. Biglieri, and V. Castellani, *Digital Transmission Theory.* Englewood Cliffs, NJ: Prentice-Hall, 1987.
[18] J. G. Proakis, *Digital Communications.* New York: McGraw-Hill, 1989.
[19] G. Ungerboeck, "Adaptive maximum likelihood receiver for carrier modulated data transmission systems," *IEEE Trans. Commun.,* vol. COM-22, pp. 624–636, May 1974.
[20] G. D'Aria and V. Zingarelli, "Results on fast-Kalman and Viterbi adaptive equalizers for mobile radio with CEPT/GSM system characteristics," in *Proc. IEEE Globecom '88,* Hollywood, FL, Nov. 28–Dec. 1, 1988.

Giovanna D'Aria was born in Italy on May 20, 1959. She received the Dr. Ing. degree in electronic engineering from the Polytechnic of Turin, Turin, Italy, in 1984.

Since 1984 she has been working as Research Engineer in the Radio Systems Department of Centro Studi e Laboratori Telecomunicazioni (CSELT), Turin. Her main interests include modulation and coding, adaptive filtering, performance evaluation, system modeling and simulation, for both fixed and mobile digital radio systems.

Flavio Muratore was born in Turin, Italy, in 1958. He received the degree in electronic engineering from the Polytechnic of Turin, Turin, Italy, in 1983.

Since 1983 he has been with the Centro Studi e Laboratori Telecomunicazioni (CSELT), Turin, where he works in the Radio Systems Department. Adaptive equalization for microwave radio-relay systems and digital satellite communications systems were the first fields he was engaged in, before becoming involved in works for the standardization of European telecommunication systems, such as the Global System for Mobile Communication (GSM), the Digital European Cordless Telecommunications (DECT) system and the pan-European Radio Message System (ERMES) of which he chaired a subtechnical committee. His current interests mainly cover mo-demodulation and co-decoding techniques, and software design for the simulation of radio chains with both TDMA and CDMA accesses. He is author of various papers on telecommunication radio aspects.

Valerio Palestini was born in Alessandria, Italy, in 1958. He received the degree in electronic engineering from the Polytechnic of Turin, Turin, Italy, in 1983.

Since then he has been with the Centro Studi e Laboratori Telecomunicazioni (CSELT), Turin, where he works in the Radio Systems Department. He has been involved in the activity of Italian cell planning for Total Access Communication System (TACS), in the studies on the Global System for Mobile Communications (GSM), digital land mobile radio system in the 900 MHz band, the pan-European Radio Message System (ERMES) and the Digital European Cordless Telecommunications (DECT) system. His main interests cover mo-demodulation methods, co-decoding techniques, interferences and outage probability in cellular coverages, dynamic channel allocation performance, and software design for the computer simulation of both TDMA and CDMA systems. He is author of various papers on the above-mentioned topics.